Strong magnetic pair breaking in Mn-substituted MgB_2 single crystals

K. Rogacki,[1,2] B. Batlogg,[1] J. Karpinski,[1] N. D. Zhigadlo,[1] G. Schuck,[1] S. M. Kazakov,[1,*] P. Wägli,[1] R. Puźniak,[3] A. Wiśniewski,[3] F. Carbone,[4] A. Brinkman,[4] and D. van der Marel[4]

[1]*Laboratory for Solid State Physics, ETH Zürich, 8093 Zürich, Switzerland*

[2]*Institute of Low Temperature and Structure Research, Polish Academy of Sciences, 50-950 Wroclaw, P.O.Box 1410, Poland*

[3]*Institute of Physics, Polish Academy of Sciences, Aleja Lotników 32/46, 02-668 Warsaw, Poland*

[4]*Département de Physique de la Matière Condensée, Universitée de Genève, 1211 Genève 4, Switzerland*

(Received 24 October 2005; revised manuscript received 7 April 2006; published 23 May 2006)

Magnetic ions (Mn) were substituted in MgB_2 single crystals resulting in a strong pair-breaking effect. The superconducting transition temperature, T_c, in $Mg_{1-x}Mn_xB_2$ has been found to be rapidly suppressed at an initial rate of 10 K/%Mn, leading to a complete suppression of superconductivity at about 2% Mn substitution. This reflects the strong coupling between the conduction electrons and the 3*d* local moments, predominantly of magnetic character, since the nonmagnetic ion substitutions, e.g., with Al or C, suppress T_c much less effectively (e.g., 0.5 K/%Al). The magnitude of the magnetic moment ($\simeq 1.7\ \mu_B$ per Mn), derived from normal state susceptibility measurements, uniquely identifies the Mn ions to be divalent, and to be in the low-spin state ($S=1/2$). This has been found also in x-ray absorption spectroscopy measurements. Isovalent Mn^{2+} substitution for Mg^{2+} mainly affects superconductivity through spin-flip scattering reducing T_c rapidly and lowering the upper critical field anisotropy H_{c2}^{ab}/H_{c2}^{c} at $T=0$ from 6 to 3.3 ($x=0.88\%$ Mn), while leaving the initial slope dH_{c2}/dT near T_c unchanged for both field orientations.

DOI: 10.1103/PhysRevB.73.174520 PACS number(s): 74.70.Ad, 74.62.Dh, 74.25.Ha, 74.25.Op

I. INTRODUCTION

Shortly after the discovery of 40 K superconductivity in MgB_2,[1] the intensive studies of its electronic structure revealed that this compound is a two-gap multi-band superconductor with two-dimensional (2D) σ-band and three-dimensional (3D) π-band.[2–5] The high superconducting transition temperature, T_c, is mainly associated with the σ-band, and T_c depends on both the electron (hole) doping intensity, which changes the Fermi level and the Fermi surface geometry,[6–8] and the interband scattering,[9–12] which may also influence the anisotropy.[13,14] On the other hand, as in conventional superconductors, T_c is expected to be affected by the pair-breaking effect caused by magnetic impurities or substitutions that suppress superconductivity due to the exchange interaction between conduction electrons and magnetic moments of the substituted ions.[15] The magnetic pair-breaking effect has been studied intensively in classic[16–22] and high-temperature superconductors,[23–27] however, this effect has remained almost untouched in more exotic superconductors, particularly in two-gap multi-band MgB_2, where no experimental and only two theoretical reports on such studies have been published.[12,15] The main goal of this work is to study the influence of magnetic Mn-ion substitutions on the normal-state and superconducting properties of high-quality MgB_2 single crystals. The results are analyzed and discussed in the context of nonmagnetic ion substitutions that affect superconductivity considerably less.

In conventional superconductors the substitution of a small amount of magnetic impurities destroys superconductivity but the addition of nonmagnetic ions is rather harmless. In unconventional multi-band multi-gap superconductors, both magnetic and nonmagnetic impurities may affect superconductivity in a similar way, depending on intraband and interband scattering. An enormous activity in experimental and theoretical studies has been performed to explain the puzzling behavior of the multi-band two-gap superconductor MgB_2 substituted with nonmagnetic ions. Here, the most intensively studied substitutions are Al for Mg (Refs. 28–32) and C for B (Refs. 33–36); both fill the MgB_2 hole-bands with electrons and also introduce scattering centers that may act in different ways. In spite of this great experimental and theoretical effort, the superconducting and normal-state properties of MgB_2 substituted with magnetic ions have been investigated briefly and in polycrystalline materials.[37–40] Concomitantly to this work, the Mn-substituted MgB_2 crystals from the same batches have been studied by a point-contact spectroscopy.[41]

In our previous studies we have reported on the crystallographic and superconducting properties of MgB_2 single crystals substituted with Al and C ions.[31,36] These electron-doping non-magnetic substitutions result in a similar moderate decrease of the superconducting transition temperature, T_c, and in a different influence on the upper critical field. In the present study we focus in detail on the crystallographic, magnetic, and superconducting properties of MgB_2 single crystals substituted with Mn ions, that act as effective magnetic scattering centers. We report a rapid reduction of T_c due to the Mn-ion substitution and, in contrast, a moderate influence of Mn on a temperature dependence of the upper critical field, H_{c2}, and the critical field anisotropy $\gamma=H_{c2}^{ab}/H_{c2}^{c}$. A central question in the discussion on the influence of Mn on superconducting properties of MgB_2 is the valence state of Mn and the spin configuration of its *d*-electrons. We have studied the magnetic state of Mn by measuring the normal state magnetization and the x-ray absorption involving the 3*d* electrons. All modifications of the superconducting properties are consistent with strong magnetic pair breaking by Mn^{2+} ions with $S=1/2$.

II. EXPERIMENTAL

Single crystals of $Mg_{1-x}Mn_xB_2$ have been grown under high pressure using the cubic anvil press. A mixture of Mg, Mn, B, and BN is placed in a BN crucible in a pyrophyllite cube. (For example, the Mg:Mn:B:BN ratio of 9.5:0.5:12:1 results in crystals with 2% of Mn substituted.) The inner diameter of the crucible is 8 mm, and its length is 8.5 mm. The heating element is a graphite tube. Six anvils generate pressure on the whole assembly. The typical growth process involves: (i) Increasing of pressure up to 30 kbar, (ii) increasing of temperature up to 1960 °C in 1 h, (iii) dwelling for 0.5–1 h, (iv) lowering the temperature and pressure in 1 h. As a result, $Mg_{1-x}Mn_xB_2$ crystals sticking together with BN crystals have been obtained. Using this method, $Mg_{1-x}Mn_xB_2$ crystals up to $0.8\times0.8\times0.1$ mm^3 have been grown. The phase purity of the crystals has been confirmed by x-ray diffraction. The Mn content has been determined by energy dispersive x-ray (EDX) analyses. For all Mn substitutions from 0.4% to 7%, the crystals are single phase and homogenous, at least within ±0.04% of Mn content.

The lattice parameters of Mn-substituted crystals were determined by a four-circle single crystal x-ray diffractometer Siemens P4 with molybdenum $K_{\alpha1}$ radiation. A set of 32 reflections recorded in the range of 2Θ angle ($15°<2\Theta<32°$) was used to calculate the unit cell parameters. Detailed structure analysis was performed for several $Mg_{1-x}Mn_xB_2$ single crystals with Mn content up to $x=0.07$. Measurements were carried out on a Bruker SMART CCD system with molybdenum $K_{\alpha1}$ radiation. The refinement of $Mg_{1-x}Mn_xB_2$ structure with Mn on Mg position was successful and no phase separation was observed.[42]

Magnetic properties in the normal and superconducting states were investigated by magnetic moment measurements performed as a function of temperature and field with a Quantum Design magnetic property measurement system (QD-MPMS) equipped with a 7 T superconducting magnet. Individual crystals with a mass of about 25 μg as well as a collection of 25 crystals with a mass of 847 μg were studied to obtain more reliable quantitative results. In order to determine the upper critical field, the magnetic moment M was measured at constant field upon heating from the zero-field-cooled state (ZFC mode) or the field-cooled state (FC mode), with a temperature sweep of 0.1 K/min. Occasionally, M was also measured at constant temperature with increasing field, using the step-by-step option. Complementary torque measurements were performed to obtain the upper critical field properties at higher fields. The torque $\tau=\mathbf{M}\times\mathbf{B}\approx\mathbf{M}\times\mathbf{H}$ was recorded as a function of the angle between the applied field and the c-axis of the crystal for various fixed temperatures and fields. For the torque measurements, a QD physical property measurement system (QD-PPMS) with torque option and a maximum field of 9 T was used. For details of torque measurements see Ref. 43.

X-ray absorption spectroscopy (XAS) measurements on the $2p$ to $3d$ absorption threshold of Mn ions in MgB_2 single crystals have been performed on the beam line BACH at "Elettra" synchrotron (Trieste).[44] The spectra have been collected both in total electron yield (TEY) and total fluorescence yield (TFY) at room temperature. The TEY technique measures the photoconductivity of the sample as a function of the incoming photon energy, this quantity is directly related to the optical absorption cross section. This method is sensitive to the first 50 Å of the sample, which means that the contamination of the surface could affect the shape of the spectrum. The TFY method measures the integrated intensity of the fluorescence decay $3d\rightarrow2p$ as a function of the incoming photon energy. This quantity is usually not one to one related to the optical absorption cross section because of self absorption and saturation phenomena. These phenomena are less important when the fluorescent ion is present at low concentrations, which makes TFY particularly suitable for studying the absorption spectra of diluted solutions or impurities in crystals.[45] The main advantage of TFY is the bulk sensitivity, probing the first 200 nm of the sample. On the other hand, TFY is experimentally more demanding, resulting in a longer acquisition time and a poorer resolution.

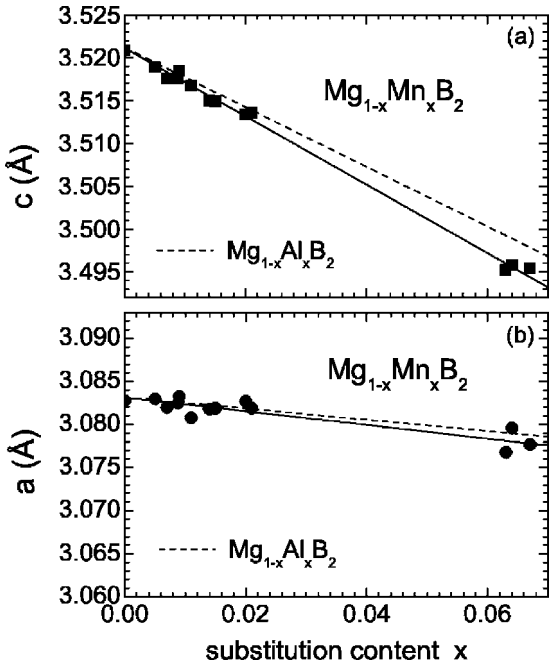

FIG. 1. Lattice parameters c and a vs Mn content x (determined with EDX) for $Mg_{1-x}Mn_xB_2$ single crystals (closed symbols, solid lines). The crystals are superconducting for $x<0.02$. The solid lines are linear fits to the data. The dashed lines represent the lattice parameters for Al-substituted crystals (Ref. 31).

III. RESULTS AND DISCUSSION

In Fig. 1 we show the lattice parameters c and a versus Mn content for $Mg_{1-x}Mn_xB_2$ single crystals with x from 0 to 0.067.[46] A significant linear decrease of $4\cdot10^{-3}$Å/%Mn of the c-axis parameter with substitution is observed. Much weaker substitution effect on the c-axis parameter was found for nearly single-phase polycrystalline $Mg_{1-x}Mn_xB_2$, where the Mn content was taken as the nominal content and thus could be overestimated.[37] The variation of the a-axis parameter with x is much smaller. Similar behavior of $c(x)$ and $a(x)$ was reported for Al-substituted crystals,[31] and for Co- and Cr-substituted polycrystalline materials.[38,40] The distinct con-

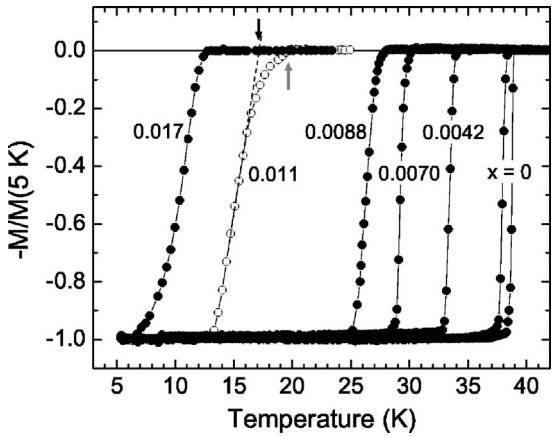

FIG. 2. Normalized magnetic moment M vs temperature for the $Mg_{1-x}Mn_xB_2$ single crystals with various Mn content x. The measurements were performed in a field of 0.5 mT, after cooling in a zero field. The superconducting transition temperature T_c is marked by a solid arrow and the transition onset temperature T_{co} by a grey arrow. Crystals with a sharp transition (closed circles) were selected for further studies.

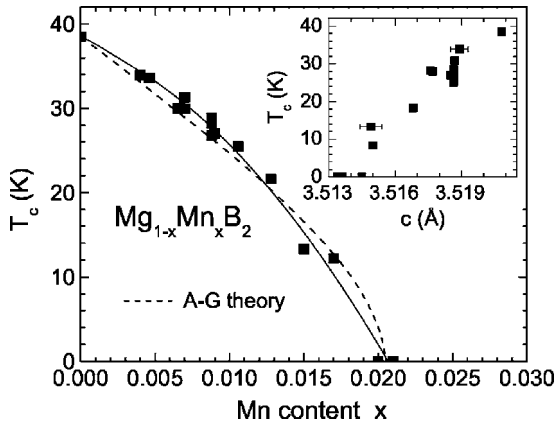

FIG. 3. Suppression of T_c with Mn substitution for $Mg_{1-x}Mn_xB_2$ single crystals with a sharp transition to the superconducting state (see Fig. 2). The solid line is a polynomial fit to the experimental points. The dashed line shows $T_c(x)$ predicted by the A-G pair-breaking theory. The inset shows T_c vs the lattice parameter c. For clarity, only two error bars are shown.

traction of the MgB_2 unit cell along the c-axis observed for our substituted crystals indicates that Mn enters the crystal structure. Similar conclusion has been also derived from the single crystal x-ray investigations where it was possible to refine the $Mg_{1-x}Mn_xB_2$ structure with Mn on Mg position only. Considering the contraction of the unit cell with Mn substitution, a simple comparison of the ionic radii of Mg and Mn suggests that the effective valence state of Mn can be 3+ with low-spin as well as high-spin configuration or 2+ with low-spin configuration only. As we will show later, the magnetic and x-ray absorption studies reveal that the Mn ions substituted for Mg are divalent and in the low-spin configuration.

The superconducting transition temperature was determined from the magnetic moment measurements performed as a function of temperature in a 0.5 mT dc field in ZFC mode. As an example, the $M(T)$ results for crystals with various Mn content are shown in Fig. 2. The effective transition temperature T_c and the onset temperature T_{co} were defined as illustrated in Fig. 2. A broad transition to the superconducting state for the crystal with $x=0.011$ is included to clearly illustrate the definitions. A difference $\Delta T_c = T_{co} - T_c$ is identified with the sample quality and it varies from 0.1 to 2.5 K at 0.5 mT, depending on the Mn content and synthesis conditions. Crystals with $\Delta T_c(0.5\ \mathrm{mT}) \leqslant 1$ K were selected for further studies.

Magnetic moment versus field has been measured to examine shielding effects and to estimate an upper limit of the superconducting volume fraction for Mn-substituted crystals. Virgin magnetization curves $M(H)$ were obtained at low temperatures for the $Mg_{1-x}Mn_xB_2$ crystals with $x=0.0088$. For a crystal with a mass of 23.5 (± 0.5) μg and dimensions $0.55 \times 0.35 \times 0.045$ mm^3, the superconducting volume fraction $f = 0.96$ (± 0.04) was derived at 10 K ($T < 0.5T_c$) with a demagnetizing factor $n=0.06$ for H parallel to the main surface of the crystal. This confirms full diamagnetism of the Mn-substituted crystal certifying its good quality. First deviation from the linear part of the $M(H)$ virgin curve was used to roughly estimate the lower critical field $\mu_o H_{c1} \simeq 19$ and 12 mT at 4.5 and 10 K, respectively, for H parallel to the ab-plane. These values signify the upward curvature of the H_{c1} versus T dependence (above 10 K at least) and are similar[47] or much lower[48,49] than those observed for unsubstituted MgB_2.

The superconducting transition temperature systematically decreases with Mn substitution resulting in a complete suppression of superconductivity at $x \simeq 0.02$, as shown in Fig. 3. The suppression is faster than linear in the whole range of doping and can be described by the magnetic pair-breaking effect. According to the Abrikosov-Gor'kov (A-G) pair-breaking theory the interaction of magnetic impurities with conduction electrons may break the time-reversal symmetry of the Cooper-pairs and result in a rapid decrease of T_c with the concentration of magnetic ions x.[50] The reduced $T_c(x)$ is well described by the relation $\ln(t_c) = \Psi(\frac{1}{2}) - \Psi(\frac{1}{2} + 0.14 t_c \alpha/\alpha_{cr})$, with $t_c = T_c(x)/T_c(0)$.[51] $\Psi(z)$ is digamma function, and α/α_{cr} is the normalized pair-breaking parameter which is identical to x/x_{cr}, where x_{cr} is the concentration of magnetic impurities required to supperss T_c to zero. The dependence of $T_c(x)/T_c(0)$ as a function of x/x_{cr} follows a universal relation. For small x, $T_c(x)$ changes roughly linearly and drops more rapidly for x closer to x_{cr}. For the Mn-substituted MgB_2 crystals, we found a very similar dependence (see Fig. 3), however, a small deviation from the A-G curve seems to be present. This possible deviation could be a result of unconventional two-gap superconductivity, where the interband scattering, which may grow with the amount of substituted magnetic ions, is postulated as an additional mechanism that reduces T_c.[9–12]

The rapid decrease of T_c caused by Mn ions is particularly clear when the Mn substitution is compared with others. In Fig. 4 we show $T_c(x)$ for MgB_2 crystals substituted with Mn for Mg, and electron-doped Al for Mg and C for B. The dramatic suppression of T_c for the Mn-substituted crystals seems to be a pure magnetic pair-breaking effect, because

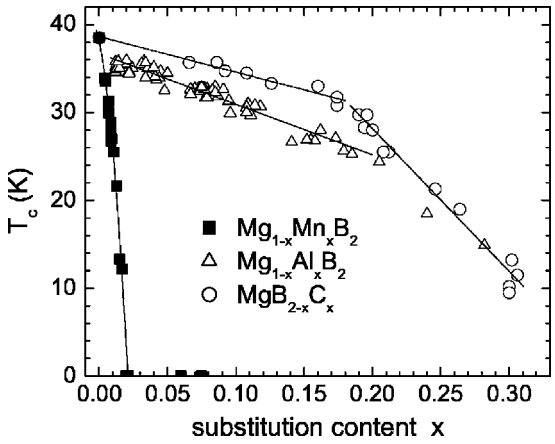

FIG. 4. Variation of T_c for MgB_2 single crystals substituted with nonmagnetic (Al, C) and magnetic (Mn) ions. The most striking result is a rapid suppression of T_c due to the substitution of isovalent Mn for Mg. The main part of the results on Al- and C-substituted crystals has been published in Refs. 31 and 36, respectively.

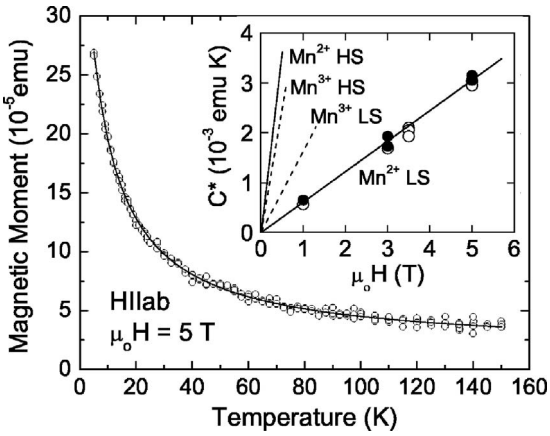

FIG. 5. Temperature dependence of the magnetic moment M at a constant field $\mu_o H=5$ T for MgB_2 single crystals substituted with 0.88% of Mn. The sample consists of 25 crystals with $T_c \simeq 28(\pm 1)$ K and a total mass of 847 μg (1.61×10^{-7} mol Mn). The inset shows the Curie part $C^\star$ of the $M(T)$ dependence as obtained from the experiment (circles). The lines are the expectations for $C^\star$ based on Mn^{2+} (solid lines) or Mn^{3+} (dashed lines) in the high-spin (HS) and low-spin (LS) configuration. The measurements reveal Mn to be divalent in the low-spin configuration. H was oriented either parallel to the *ab*-plane (open circles) or 70° off the *ab*-plane (solid circles).

any essential changes of the electronic structure are not expected for the reason that Mn substitutes as isovalent Mn^{2+}, as we discuss below. This requires strong interaction between the localized $3d$ electrons of Mn and conduction (mostly) $2s2p$ electrons of B even if we realize that the magnetic impurities are located at the Mg sites, which are spatially separated from the B planes. A large difference between the T_c suppression rates for magnetic and nonmagnetic substitutions is consistent with orthogonality of the σ and π orbitals and, consequently, with the much smaller interband than intraband scattering.[52] An interesting issue is if so fine substitution of Mn for Mg, which yet changes T_c so rapidly, modifies the σ and π intraband scattering and influences the σ-band anisotropy. This we discuss in the paragraphs devoted to properties of the upper critical field.

The normal state magnetization was measured on individual single crystals (typically $m\simeq 25$ μg) and on an assembly of 25 crystals (0.88% Mn, total $m\simeq 847$ μg) attached with vacuum grease to a nonmagnetic sample holder. The presence of Mn ions manifests itself in a Curie-Weiss contribution that dominates $M(T)$ even at the low Mn concentrations of $<1\%$. An example of the $M(T)$ dependence is shown in Fig. 5 for the multi-crystal assembly. For individual crystals, $M(H)$ curves were measured at various temperatures to calculate $M(T)$, since the small crystal mass and the low Mn content resulted in $\sim 10^{-8}-10^{-7}$ mol Mn. The normal state magnetic moment was analyzed according to the formula $M(T)=M_o+C^\star/(T+\Theta)$, where $C^\star/(T+\Theta)$ is the Curie-Weiss contribution associated with the Mn local moments. The effective interaction temperature Θ is found to be $\leqslant 2$ K, reflecting the high dilution of the Mn ions. The value of $C^\star$ is shown in the inset of Fig. 5 for $M(T)$ measurements in fields up to 5 T, and for H either parallel to or 70° off the crystal *ab*-plane. $C^\star(H)$ is isotropic within the measurement limits and grows linearly with H, as expected.

The magnitude of the local-moment Curie-Weiss part of $M(T)$ reveals unambiguously that Mn in MgB_2 is in the divalent state, isovalent to Mg. The lines in the inset of Fig. 5 are the calculated values of $C^\star(H)$, assuming Mn^{2+} and Mn^{3+}, in either high-spin or low-spin state. The measured data, which correspond to $m_m\simeq 1.7$ μ_B per Mn ion, are in excellent agreement with low-spin Mn^{2+}, and they are clearly distinct from the alternative states. Thus, we conclude that the crystal field acting upon the d electrons is strong enough to produce a low-spin configuration with an effective $S=1/2$. Measurements on other crystals, including one with 6.5% Mn, lead to the same conclusion.

Information on the d-electron configuration can be deduced also from x-ray absorption spectroscopy (XAS). The $2p$ to $3d$ XAS spectrum in transition metals has been proved to be a sensitive probe to their electronic ground state.[53] It is possible to calculate the XAS spectrum with a standard Cowan code,[54] based on an atomic model, and compare it to the experimental spectra. This approach is very suitable for the determination of the valency of transition metal impurities in crystals. In Fig. 6 we show the experimental TEY and TFY spectra (see Experimental) together with the atomic model calculations without and with a cubic crystal field, which mimics the presence of the solid around the Mn ion. In the upper panel of Figure 6 the TEY spectrum shows the typical shape of the high-spin Hund's rule ground state. The TFY measurements, though the resolution does not allow to distinguish very clear features, show a shoulder on the low energy side of the L_2 edge and a shift of the white line by about 2 eV towards higher energies. In the lower panel we plot three simulations of the Mn^{2+} XAS spectrum without considering any crystal field and with a cubic crystal field just above the high-spin to low-spin transition value, which for Mn is around 2.4 eV. The ligand field value at the Mn site has been obtained performing a band calculation assum-

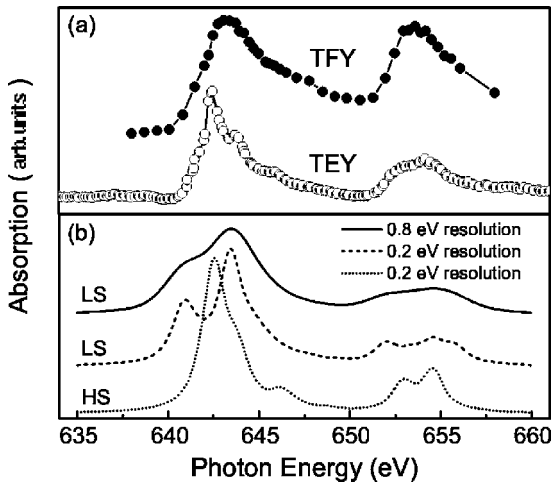

FIG. 6. (a) XAS spectra for the TEY and the TFY experiments on MgB_2 single crystals substituted with 6.7% of Mn. In the TEY mode, the spectrum is probably dominated by a MnO surface layer, while the TFY mode is more sensitive to the bulk. (b) Atomic model calculations for the $3d^5$ ground state of Mn in the low-spin (LS) and high-spin (HS) configuration. All the curves are shifted for clarity.

ing the MgB_2 crystal structure and replacing all the Mg atoms with Mn atoms; this calculation gives a crystal field value of about 2 eV, which as a first approximation is close enough to the value necessary to induce the high-spin to low-spin transition in Mn. The effect of the crystal field on the spectrum is to shift the white line at higher energies by an amount which is related to the crystal field value itself; a peak on the low energy side of the spectrum also arises, which in a spectrum with lower resolution becomes a pronounced shoulder. Our interpretation is that the Mn present on the surface is probably oxidized, giving to the TEY spectrum the typical shape of the high-spin ground state. The surface contamination of MgB_2 when crystals are exposed to air has already been pointed out with optical experiments.[55] However, the TFY spectrum reveals the bulk properties of the sample, suggesting that the Mn^{2+} ions are in a low-spin configuration induced by the crystal field effect. This result is consistent with our magnetic measurements, discussed above.

The upper critical field, H_{c2}, has been determined from magnetic moment measurements performed as a function of temperature at constant field or versus field at constant temperature. In Fig. 7 we show examples of $M(T)$ and $M(H)$ results for the crystal substituted with 0.88% of Mn. The results have been obtained with a field oriented parallel, H^{ab}, and perpendicular, H^c, to the *ab*-plane. The superconducting transition temperature T_c and the transition onset temperature T_{co} have been defined as shown in Fig. 7. The difference between T_c and T_{co} obviously depends on the field orientation and value, however this modifies the $H_{c2}(T)$ results only slightly (see Fig. 8). Extensive sets of data similar to these presented in Fig. 7 are analyzed to construct the $H_{c2}-T$ phase diagram. Figure 8 shows the upper critical field of the $Mg_{1-x}Mn_xB_2$ crystals with $x=0.0042$ and 0.0088, and, for comparison, of the unsubstituted compound. For the heavily

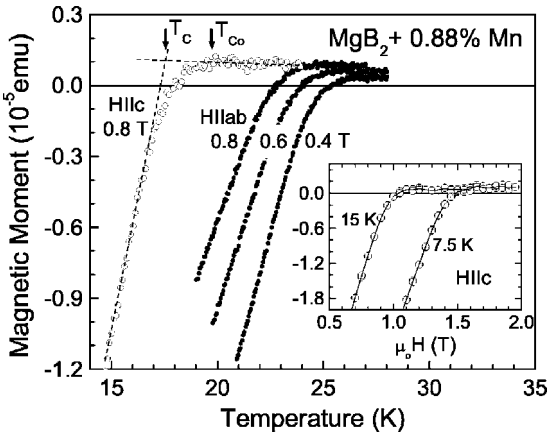

FIG. 7. Diamagnetic response of the MgB_2 crystal substituted with 0.88% of Mn. Shown are examples of measurements in constant field or at constant temperature (inset), for the two main orientations of the field. The transition temperature T_c and the transition onset temperature T_{co} are marked by arrows.

doped crystal, special attention has been paid to obtain accurate H_{c2} values at low fields to determine the upper critical field slope, dH_{c2}/dT, near T_c. For this crystal ($x=0.0088$, $T_c=26.8$ K), $d\mu_o H_{c2}/dT$ at T_c is equal to $-0.205(\pm 0.005)$ and $-0.100(\pm 0.005)$ T/K, for H oriented parallel and perpendicular to the *ab*-plane, respectively. These values are practically the same as for unsubstituted crystals: -0.21 and -0.10 T/K, respectively.

According to the quasi-classic model of the two-band superconductor in the dirty limit (without magnetic impurities), the temperature dependence of H_{c2} close to T_c is determined by the intraband scattering for the band with a maximum

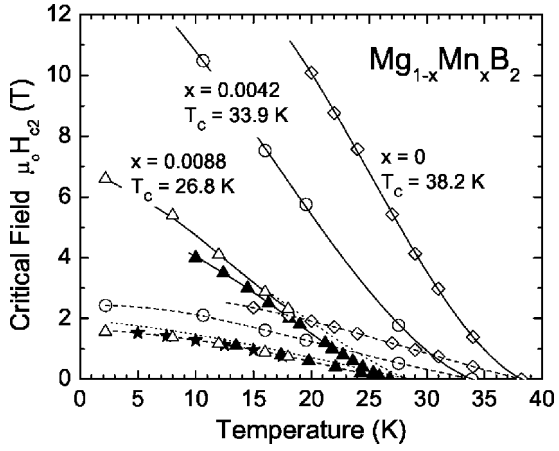

FIG. 8. Upper critical field H_{c2} vs temperature for the $Mg_{1-x}Mn_xB_2$ single crystals with $x=0$ (diamonds), 0.0042 (circles), and 0.0088 (triangles, stars). The $H_{c2}(T)$ data were obtained by magnetization measurements (solid symbols) or derived from torque measurements (open symbols), for the magnetic field H oriented parallel (solid lines) and perpendicular (dashed lines) to the *ab*-plane. The magnetization measurements were performed at constant H with increasing T (solid triangles) or at constant T with increasing H (stars). The doted lines show the $H_{c2}(T)$ corresponding to the transition onset temperature T_{co} (see Fig. 7). The lines are a guide for the eye.

diffusivity, when assumed that the intraband and interband electron-phonon coupling constants are finite.[56,57] For pure MgB_2, the band with a maximum diffusivity is the π-band.[52,58,59] Thus, the unchanged dH_{c2}/dT, observed for the Mn-substituted MgB_2 crystals close to T_c, suggests that the π-band diffusivity (or scattering) is not affected by the low-level substitution of magnetic isovalent ions for Mg. As a consequence, the diffusivity in the π-band remains dominant and the upper critical field at zero temperature, $H_{c2}(0)$, should be determined by T_c and the minimum diffusivity,[57] i.e., the diffusivity in the σ-band. A roughly linear $H_{c2}(0) - T_c$ relation is observed for the Mn-substituted crystals. Thus, the Mn substitution causes merely minimal changes in the π-band and the σ-band diffusivity, and suppresses T_c by spin-flip scattering. Similar conclusions have been drawn from a point-contact spectroscopy.[41]

There are at least two mechanisms possible for the reduction of T_c in MgB_2 substituted with magnetic isovalent ions. One is the impurity-induced (nonmagnetic) interband scattering and the second is the magnetic pair-breaking effect. The interband scattering alone is expected to reduce T_c at most to about 25 K and, most likely, for the amount of substituted ions much higher than 2%,[10,11] that for the Mn-substituted crystals suppresses T_c to zero. Moreover, any significant modification of the interband scattering requires a substantial concentration of the impurity ions in the B plane rather than in the Mg plane,[52,60,61] as shown for C-substituted MgB_2.[11,62] Thus, the main mechanism that controls T_c in the Mn-substituted MgB_2 remains the magnetic pair-breaking effect.

The overall temperature dependence of H_{c2} is characterized mainly by a reduction of the scales when Mn is substituted. In particular, the anisotropy remains well pronounced, and so does the marked up-turn of H_{c2}^{ab} below T_c, which means that the two-band character determining $H_{c2}(T)$ is essentially unaffected by Mn substitution. This is in line with the above-noted unchanged initial slope of dH_{c2}/dT. In Fig. 9 we show the temperature dependence of the upper critical field anisotropy, $\gamma = H_{c2}^{ab}/H_{c2}^{c}$, for the MgB_2 single crystals substituted with 0.42% and 0.88% of Mn. For comparison, the anisotropy for nonsubstituted, Al-substituted, and C-substituted crystals is also presented. At low temperatures, a large reduction of γ from 6 to 3.3 is observed for the crystal with 0.88% of Mn. Along with the lowering of γ, its temperature dependence weakens. This behavior, observed for the MgB_2 crystals substituted with magnetic isovalent Mn^{2+}, is similar to that obtained for the crystals substituted with electron-adding Al^{3+}. Similar $\gamma(T)$ dependencies are observed for crystals with similar T_c's but with much different Mn and Al contents (lower substitution) or for crystals with significantly different T_c's (heavier substitution, see Fig. 9). For example, 0.42% ($\sim$1%) of substituted Mn results in changes similar to those observed for 2.4% ($\sim$9%) of substituted Al. Thus, the mechanism that is responsible for the reduction of the anisotropy and for changes of its temperature dependence has to be different in the both cases. Note, that the temperature dependence of γ obtained for the Mn- and Al-substituted crystals differs significantly from that derived for the C-substituted crystals. This we discuss shortly in the next paragraph.

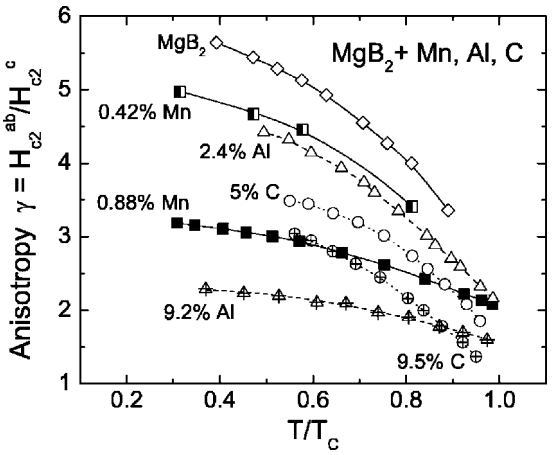

FIG. 9. Upper critical field anisotropy vs reduced temperature for the MgB_2 unsubstituted single crystals (diamonds; T_c=38.2 K) and substituted with Mn (squares; 0.42% Mn, T_c=33.9 K; 0.88% Mn, T_c=26.8 K), Al (triangles; 2.4% Al, 35.3 K; 9.2% Al, 32.0 K), and C (circles; 5% C, 34.3 K; 9.5% C, 30.1 K). The data for Al- and C-substituted crystals were derived from $H_{c2}(T)$ results published in Refs. 31 and 36.

The upper critical field anisotropy decreases with increasing temperature for both unsubstituted and substituted crystals, as shown in Fig. 9. For a weak-coupling multiband BCS model for two-gap superconductors (without magnetic impurities), a negative anisotropy slope, $d\gamma/dT$, is expected for the case when diffusivity in the π-band dominates.[57] This requirement seems to be fulfilled in the clean nonsubstituted or C-substituted MgB_2, where C on the B position decreases the diffusivity mainly in the σ-band, as shown for C-substituted single crystals[63] and epitaxial thin films.[64] Thus, the negative slope $d\gamma/dt$, which at lower temperatures ($t=T/T_c \leqslant 0.5$) is similar for nonsubstituted and C-substituted crystals (see Fig. 9), is fully consistent with this prediction. On the other hand, when the diffusivity in the σ-band dominates, $\gamma(T)$ is expected to be less temperature dependent, or $d\gamma/dt$ may even become positive.[57,65] The diffusivity in the σ-band may dominate, when the scattering in the π-band increases substantially, e.g., due to the substitution of Al for Mg.[66] Both Mn and Al substitutions show a tendency to lower $|d\gamma/dt|$ with the increasing amount of substituted ions. For an unsubstituted crystal (T_c=38.2 K), $|d\gamma/dt|$=2.6 at t=0.4 and decreases slightly to about 2.3, for the crystals with 0.42% of Mn (T_c=33.9 K) or 2.4% of Al (T_c=35.3 K), and more significantly to 0.91 and 0.42, for the crystals with 0.88% of Mn (T_c=26.8 K) and 9.2% of Al (T_c=32.0 K), respectively.

For the Al-substituted crystals, the observed suppression of $|d\gamma/dt|$ can be interpreted as a result of increased intraband scattering in the π-band.[66] For the Mn-substituted crystals, the explanation seems to be different, as dH_{c2}/dT at T_c remains unchanged. Here, pair breaking due to spin-flip scattering appears to dominate the reduction of T_c and the H_{c2} anisotropy. A reduction of the energy gap due to spin-flip scattering is expected to be different for both bands and thus the ratio Δ_σ/Δ_π may vary with temperature in a way that is different from that in unsubstituted MgB_2. The details can be

worked out through T-dependent gap spectroscopy revealing changes in the magnitude and weakening of the temperature dependence of Δ_σ and Δ_π due to spin-flip scattering. Such spectroscopic studies may also reveal if some of the scenarios discussed theoretically for magnetic pair breaking in MgB_2 apply to this compound.[15]

IV. CONCLUSIONS

We have studied the influence of Mn substitution on the superconducting properties of MgB_2 by growing single crystals with Mn concentrations up to 7%, and measuring their magnetic properties and x-ray absorption spectra. Mn suppresses T_c very effectively at an initial rate of ~ 10 K/%Mn, and T_c is fully suppressed at $\simeq 2\%$ of Mn. The temperature dependence of $H_{c2}(T)$ and $\gamma(T)$ obtained for the Mn-substituted single crystals is similar to that reported previously for MgB_2 substituted with nonmagnetic Al, provided that the crystals with similar T_c are compared. This suggests that in MgB_2, where Mg is substituted with magnetic or nonmagnetic ions, the main parameter that controls both $H_{c2}(T)$ and $\gamma(T)$ is the superconducting transition temperature, irrespective of the mechanism responsible for the T_c suppression. For Mn-substituted MgB_2, this suppression is found to be due to the magnetic pair-breaking effect caused by Mn ions, as Mn substitutes for Mg isovalently as Mn^{2+} in the low-spin ($S=1/2$) configuration. Along with the reduction of T_c, the upper critical field $H_{c2}(0)$ and its anisotropy are also reduced, while the initial slope dH_{c2}/dT near T_c and the associated anisotropy remain essentially unaffected. These results suggest that the magnetic Mn substitution predominantly influences the superconducting properties through spin-flip scattering, leaving the diffusivity in the σ and π bands largely unaffected. A further treatment will have to include the detailed knowledge of the influence of magnetic pair breaking on the σ and π bands in MgB_2 and the resulting modification of the electronic properties of this two-gap superconductor.

ACKNOWLEDGMENTS

This work was supported in part by the Swiss National Science Foundation, MaNEP, the Center of Excellence (CELTAM) established under the Grant No. GMA1-2002-72017 within 5th Framework Program of European Community (Contract No. G5MA-CT.2002.04032) (K.R.), and the Polish State Committee for Scientific Research under a research project for the years 2004–2006 (1 P03B 037 27) (R.P. and A.W.). The SMART CCD measurements were performed at the Laboratory of Inorganic Chemistry, ETH Zurich.

*Present address: Department of Chemistry, Moscow State University, 119899 Moscow, Russia.

[1] J. Nagamatsu, N. Nakagawa, T. Muranaka, Y. Zenitani, and J. Akimitsu, Nature (London) **410**, 63 (2001).
[2] J. Kortus, I. I. Mazin, K. D. Belashchenko, V. P. Antropov, and L. L. Boyer, Phys. Rev. Lett. **86**, 4656 (2001).
[3] A. Y. Liu, I. I. Mazin, and J. Kortus, Phys. Rev. Lett. **87**, 087005 (2001).
[4] H. J. Choi, D. Roundy, H. Sun, M. L. Cohen, and S. G. Louie, Nature (London) **418**, 758 (2002).
[5] For a review, see P. C. Canfield and G. W. Crabtree, Phys. Today **56**, 34 (2003).
[6] O. de la Peña, A. Aguayo, and R. de Coss, Phys. Rev. B **66**, 012511 (2002).
[7] D. Kasinathan, K.-W. Lee, and W. E. Pickett, Physica C **424**, 116 (2005).
[8] R. F. Klie, J. C. Zheng, Y. Zhu, A. J. Zambano, and L. D. Cooley, Phys. Rev. B **73**, 014513 (2006).
[9] A. A. Golubov, J. Kortus, O. V. Dolgov, O. Jepsen, Y. Kong, O. K. Andersen, B. J. Gibson, K. Ahn, and R. K. Kremer, J. Phys.: Condens. Matter **14**, 1353 (2002).
[10] B. Mitrović, J. Phys.: Condens. Matter **16**, 9013 (2004).
[11] J. Kortus, O. V. Dolgov, R. K. Kremer, and A. A. Golubov, Phys. Rev. Lett. **94**, 027002 (2005).
[12] O. V. Dolgov, R. K. Kremer, J. Kortus, A. A. Golubov, and S. V. Shulga, Phys. Rev. B **72**, 024504 (2005).
[13] A. A. Golubov and I. I. Mazin, Phys. Rev. B **55**, 15146 (1997).
[14] M. Angst, S. L. Bud'ko, R. H. T. Wilke, and P. C. Canfield, Phys. Rev. B **71**, 144512 (2005).
[15] C. P. Moca and C. Horea, Phys. Rev. B **66**, 052501 (2002).
[16] For a review, see Ø. Fischer, Appl. Phys. **16**, 1 (1978).
[17] For a review, see K. N. Shrivastava and K. P. Sinha, Phys. Rep. **115**, 93 (1984).
[18] A. I. Goldman, C. Stassis, P. C. Canfield, J. Zarestky, P. Dervenagas, B. K. Cho, D. C. Johnston, and B. Stemlieb, Phys. Rev. B **50**, R9668 (1994).
[19] J. A. Chervenak and J. M. Valles, Phys. Rev. B **51**, 11977 (1995).
[20] A. Bill, S. A. Wolf, Yu. N. Ovchinnikov, and V. Z. Kresin, Physica C **298**, 231 (1998).
[21] G. Ghosh, A. D. Chinchure, R. Nagarajan, C. Godart, and L. C. Gupta, Phys. Rev. B **63**, 212505 (2001).
[22] Chang-An Kim and B. K. Cho, Phys. Rev. B **66**, 214501 (2002).
[23] G. Xiao, M. Z. Cieplak, J. Q. Xiao, and C. L. Chien, Phys. Rev. B **42**, 8752 (1990).
[24] P. Szabó, P. Samuely, A. G. M. Jansen, J. Marcus, and P. Wyder, Phys. Rev. B **62**, 3502 (2000).
[25] A. K. Chattopadhyay, R. A. Klemm, and D. Sa, J. Phys.: Condens. Matter **14**, L577 (2002).
[26] A. Poddar and B. Chattopadhyay, Eur. Phys. J. B **35**, 69 (2003).
[27] K. Rogacki, Phys. Rev. B **68**, 100507(R) (2003).
[28] J. S. Slusky, N. Rogado, K. A. Regan, M. A. Hayward, P. Khalifah, T. He, K. Inumaru, S. M. Loureiro, M. K. Haas, H. W. Zandbergen, and R. J. Cava, Nature (London) **410**, 343 (2001).
[29] R. J. Cava, H. W. Zandbergen, and K. Inumaru, Physica C **385**, 8 (2003).
[30] M. Putti, M. Affronte, P. Manfrinetti, and A. Palenzona, Phys. Rev. B **68**, 094514 (2003).
[31] J. Karpinski, N. D. Zhigadlo, G. Schuck, S. M. Kazakov, B. Bat-

logg, K. Rogacki, R. Puzniak, J. Jun, E. Müller, P. Wägli, R. Gonnelli, D. Daghero, G. A. Ummarino, and V. A. Stepanov, Phys. Rev. B **71**, 174506 (2005).
[32] A. J. Zambano, A. R. Moodenbaugh, and L. D. Cooley, Supercond. Sci. Technol. **18**, 1411 (2005).
[33] A. Bharathi, S. J. Balaselvi, S. Kalavathi, G. L. N. Reddy, V. S. Sastry, Y. Hariharan, and T. S. Radhakrishnan, Physica C **370**, 211 (2002).
[34] S. Lee, T. Masui, A. Yamamoto, H. Uchiyama, and S. Tajima, Physica C **397**, 7 (2003).
[35] T. Masui, S. Lee, and S. Tajima, Phys. Rev. B **70**, 024504 (2004).
[36] S. M. Kazakov, R. Puzniak, K. Rogacki, A. V. Mironov, N. D. Zhigadlo, J. Jun, Ch. Soltmann, B. Batlogg, and J. Karpinski, Phys. Rev. B **71**, 024533 (2005).
[37] S. Xu, Y. Moritomo, K. Kato, and A. Nakamura, J. Phys. Soc. Jpn. **70**, 1889 (2001).
[38] M. Kühberger and G. Gritzner, Physica C **370**, 39 (2002).
[39] S. X. Dou, S. Soltanian, Y. Zhao, E. Getin, Z. Chen, O. Shcherbakova, and J. Horvat, Supercond. Sci. Technol. **18**, 710 (2005).
[40] H. Zhang, J. Zhao, and L. Shi, Physica C **424**, 79 (2005).
[41] R. S. Gonnelli, D. Daghero, G. A. Ummarino, A. Calzolari, M. Tortello, V. A. Stepanov, N. D. Zhigadlo, K. Rogacki, and J. Karpinski, cond-mat/0510329 (unpublished).
[42] For details, see G. Schuck *et al.* (in preparation).
[43] M. Angst, R. Puzniak, A. Wisniewski, J. Jun, S. M. Kazakov, J. Karpinski, J. Roos, and H. Keller, Phys. Rev. Lett. **88**, 167004 (2002).
[44] M. Zangrando, M. Finazzi, G. Paolucci, G. Comelli, B. Diviacco, R. P. Walker, D. Cocco, and F. Parmigiani, Rev. Sci. Instrum. **72**, 1313 (2001).
[45] F. M. F. de Groot, M. A. Arrio, Ph. Sainctavit, Ch. Cartier, and C. T. Chen, Solid State Commun. **92**, 991 (1994).
[46] For the crystallographic structure see Ref. 1.
[47] M. Zehetmayer, M. Eisterer, J. Jun, S. M. Kazakov, J. Karpinski, A. Wisniewski, and H. W. Weber, Phys. Rev. B **66**, 052505 (2002).
[48] G. K. Perkins, J. Moore, Y. Bugoslavsky, L. F. Cohen, J. Jun, S. M. Kazakov, J. Karpinski, and A. D. Caplin, Supercond. Sci. Technol. **15**, 1156 (2002).
[49] L. Lyard, P. Szabó, T. Klein, J. Marcus, C. Marcenat, K. H. Kim, B. W. Kang, H. S. Lee, and S. I. Lee, Phys. Rev. Lett. **92**, 057001 (2004).
[50] A. A. Abrikosov and L. P. Gor'kov, ZETF **39**, 1781 (1960) , [Sov. Phys. JETP **12**, 1243 (1961)].
[51] R. D. Parks, in *Superconductivity*, edited by P. R. Wallace (Gordon and Breach, New York, 1969), Vol. 2, 625.
[52] I. I. Mazin, O. K. Andersen, O. Jepsen, O. V. Dolgov, J. Kortus, A. A. Golubov, A. B. Kuz'menko, and D. van der Marel, Phys. Rev. Lett. **89**, 107002 (2002).
[53] B. T. Thole, R. D. Cowan, G. A. Sawatzky, J. Fink, and J. C. Fuggle, Phys. Rev. B **31**, 6856 (1985).
[54] R. D. Cowan, *The Theory of Atomic Structure and Spectra* (University of California Press, Berkeley, 1981).
[55] V. Guritanu, A. B. Kuzmenko, D. van der Marel, S. M. Kazakov, N. D. Zhigadlo, and J. Karpinski, Phys. Rev. B **73**, 104509 (2006).
[56] H. Suhl, B. T. Matthias, and L. R. Walker, Phys. Rev. Lett. **3**, 552 (1959).
[57] A. Gurevich, Phys. Rev. B **67**, 184515 (2003).
[58] M. Putti, V. Braccini, E. Galleani d'Agliano, F. Napoli, I. Pallecchi, A. S. Siri, P. Manfrinetti, and A. Palenzona, Phys. Rev. B **67**, 064505 (2003).
[59] M. Putti, V. Braccini, E. Galleani, F. Napoli, I. Pallecchi, A. S. Siri, P. Manfrinetti, and A. Palenzona, Supercond. Sci. Technol. **16**, 188 (2003).
[60] S. C. Erwin and I. I. Mazin, Phys. Rev. B **68**, 132505 (2003).
[61] See also the discussion in, P. Samuely, P. Szabo, P. C. Canfield, and S. L. Bud'ko, Phys. Rev. Lett. **95**, 099701 (2005); J. Kortus, O. V. Dolgov, R. K. Kremer, and A. A. Golubov, *ibid.* **95**, 099702 (2005).
[62] R. S. Gonnelli, D. Daghero, A. Calzolari, G. A. Ummarino, V. Dellarocca, V. A. Stepanov, S. M. Kazakov, N. Zhigadlo, and J. Karpinski, Phys. Rev. B **71**, 060503(R) (2005).
[63] A. V. Sologubenko, N. D. Zhigadlo, S. M. Kazakov, J. Karpinski, and H. R. Ott, Phys. Rev. B **71**, 020501(R) (2005).
[64] I. Pallecchi, V. Ferrando, E. Galleani D'Agliano, D. Marré, M. Monni, M. Putti, C. Tarantini, F. Gatti, H. U. Aebersold, E. Lehmann, X. X. Xi, E. E. G. Haanappel, and C. Ferdeghini, Phys. Rev. B **72**, 184512 (2005).
[65] V. G. Kogan and N. V. Zhelezina, Phys. Rev. B **69**, 132506 (2004).
[66] A. Carrington, J. D. Fletcher, J. R. Cooper, O. J. Taylor, L. Balicas, N. D. Zhigadlo, S. M. Kazakov, J. Karpinski, J. P. H. Charmant, and J. Kortus, Phys. Rev. B **72**, 060507(R) (2005).